J|A|C|S
ARTICLES

Published on Web 12/03/2009

Single Amino Acid Replacement Makes *Aequorea victoria* Fluorescent Proteins Reversibly Photoswitchable

Ranieri Bizzarri,*[,†,‡] Michela Serresi,[†] Francesco Cardarelli,[†] Stefania Abbruzzetti,[‡,§] Barbara Campanini,[¶] Cristiano Viappiani,[‡,§] and Fabio Beltram[†,‡]

IIT@NEST, Center for Nanotechnology Innovation, Piazza San Silvestro 12, I-56127 Pisa, Italy, NEST, Scuola Normale Superiore and CNR-INFM, Piazza San Silvestro 12, I-56127 Pisa, Italy, Dipartimento di Fisica, Università di Parma, viale G. P. Usberti 7A, 43100 Parma, Italy, and Dipartimento di Biochimica e Biologia Molecolare, Università di Parma, viale G. P. Usberti 23A, 43100 Parma, Italy

Received February 26, 2009; E-mail: r.bizzarri@sns.it

Abstract: Reversibly photoswitchable (i.e., photochromic) fluorescent proteins open the way to a number of advanced bioimaging techniques applicable to living-cell studies such as sequential photolabeling of distinct cellular regions, innovative FRET schemes, or nanoscopy. Owing to the relevance of fluorescent proteins from *Aequorea victoria* (AFPs) for cell biology, a photochromic "toolbox" constituted by several AFPs is highly desirable. Here we introduce four new photochromic AFPs whose reversible photoswitching occurs between the native bright and a dark state at low illumination power, on account of a very efficient *cis*−*trans* photoisomerization. Most remarkably, the optical bistability of these AFPs derives from the single E222Q mutation in the primary sequence. Apparently, the E222Q substitution can restore the intrinsic photochromic behavior of the isolated chromophore. The significance of these mutants for high-resolution in vivo cell imaging is shown by means of photochromic FRET experiments.

Introduction

Fluorescent proteins (FPs) from marine invertebrates have become invaluable tools for in vivo imaging of cells and tissues. Indeed, they provide genetic encoding of bright visible fluorescence, thus enabling the noninvasive analysis of protein localization and dynamics in living cells.[1,2] Mutational strategies of the amino acid sequences of archetypal FPs yielded several variants with different spectral emission, photophysical properties, and aggregation states.[3] The most popular FPs derive from the *Aquorea victoria* jellyfish (AFP class). AFP variants display, in general, good photostability, true monomeric form, often high brightness, and are the components of most intracellular indicators based on fluorescent proteins.[3] Actually, the library of eukaryotic proteins fused to AFPs already includes hundreds of components.[2] Thus, engineering of AFP properties by selected mutations in the primary sequence represents an efficient way to modify the fluorescent reporter(s) of existing chimerae and thereby tailor the constructs to the desired imaging applications.

Recently, a novel approach to in vivo imaging emerged with the development of new fluorescent proteins that can be reversibly or irreversibly photoconverted between two optical states (photoactivatable fluorescent proteins, PAFPs).[4] PAFPs add a new temporal dimension to protein imaging techniques at the intracellular level.[1,4,5] The most impressive results are obtainable by using reversible PAFPs (photochromic FPs), as they allow repeated activation events, thus prolonging the observation of biological dynamics, and the photolabeling of several subcellular regions one after the other.[6] Furthermore, photochromic FPs stand as excellent fluorescent probes for super-resolution imaging techniques such as RESOLFT that are based on the regioselective activation/deactivation of emissive states at the nanoscale.[7] The most popular photochromic FP is Dronpa, a mutant from Pectiniidae family that can be switched several times between a bright green fluorescent state and a dark UV/violet absorbing state with only a minor loss of emission.[8] The reversible photoswitching of Dronpa has been rationalized on account of a four-state scheme entailing the isomerization of the chromophore between a *cis* anionic bright state and a *trans* neutral dark state,[9] although some authors attributed the bright−dark conversion to an increase of β-barrel flexibility.[10]

Owing to the broad applications of AFPs in cell biology, a photochromic "toolbox" constituted by stable, fast, and fully optimized photoswitchable AFPs of different colors represents

[†] IIT@NEST.
[‡] NEST, Scuola Normale Superiore and CNR-INFM.
[§] Dipartimento di Fisica, Università di Parma.
[¶] Dipartimento di Biochimica e Biologia Molecolare, Università di Parma.

(1) Chudakov, D. M.; Lukyanov, S.; Lukyanov, K. A. *Trends Biotechnol.* **2005**, *23*, 605–613.
(2) Miyawaki, A. *Neuron* **2005**, *48*, 189–199.
(3) Shaner, N. C.; Steinbach, P. A.; Tsien, R. Y. *Nat. Methods* **2005**, *2*, 905–909.
(4) Lukyanov, K. A.; Chudakov, D. M.; Lukyanov, S.; Verkhusha, V. V. *Nat. Rev. Mol. Cell Biol.* **2005**, *6*, 885–891.
(5) Lippincott-Schwartz, J.; Altan-Bonnet, N.; Patterson, G. H. *Nat. Cell Biol.* **2003**, S7–S14.
(6) Ando, R.; Mizuno, H.; Miyawaki, A. *Science* **2004**, *306*, 1370–1373.
(7) Hofmann, M.; Eggeling, C.; Jakobs, S.; Hell, S. W. *Proc. Natl. Acad. Sci. U.S.A.* **2005**, *102*, 17565–17569.
(8) Habuchi, S.; Ando, R.; Dedecker, P.; Verheijen, W.; Mizuno, H.; Miyawaki, A.; Hofkens, J. *Proc. Natl. Acad. Sci. U.S.A.* **2005**, *102*, 9511–9516.

a very significant scientific goal. We recently showed[11] that synthetic chromophores isolated from AFPs possess a reversible *cis*−*trans* photoisomerization mechanism similar to that reported for photochromic FPs from Dronpa and other sea organisms.[6,12] Notably less than 10 absorbed photons are enough to promote the structural switch in these molecules.[11] In spite of the generality of this property in isolated chromophores, reversible switching of AFPs was demonstrated only for the case of yellow variants EYFP[13] (and its alternative form 10C[14]), T203F,[13] and F64L/S65T/T203Y GFP (named E2GFP).[15] These mutants offer, however, far from optimal properties since they need to absorb on average $\sim 10^6$ photons to carry out the on−off photoconversion,[13,15] and their photochromic behavior was often reported to be accompanied by undesirable effects (e.g., irreversible photobleaching[14,16]). Nonetheless, EYFP photochromicity made it possible to obtain remarkable sub-40 nm resolution images in bacteria.[17]

On account of the general photochromic behavior of AFP chromophores, we believe that the emergence of photochromic properties in the folded protein must be regulated by the subtle interactions between the chromophore and its environment, which may, or may not, allow the *cis*−*trans* isomerization to take place. In this perspective, we set out to generate enhanced photochromic AFP variants starting from our knowledge of how the residues around the chromophore affect the photophysical properties of the proteins. E222 is a key amino acid from this point of view. A fast proton transfer between the chromophore and E222 takes place in many AFPs, and it encompasses a complex H-bond network in the ground and/or excited state.[18] This internal proton transfer is often associated with structural rearrangement of the chromophore's pocket,[18,19] which in turn could interfere with the intrinsic photochromicity of the chromophore. Additionally, *cis*−*trans* photoisomerization was demonstrated to be associated with an intramolecular charge-transfer intermediate whose progression to the *trans* state is strongly affected by H-bonding with surrounding molecules.[20]

In this work, we investigate the effect of E222 replacement on the photoconversion properties of AFPs. We shall demonstrate that the single E222Q mutation confers efficient photochromicity to four AFPs otherwise differing in mutation pattern, emission color, and ground-state photophysics. E222Q, therefore, emerges as a point mutation capable of restoring reversible photoswitching to the AFP chromophore in the complete folded protein. Moreover, E222Q prevents the frequently observed irreversible photoconversion of AFPs by E222 decarboxylation.[21,22] The significance of these mutants for high-resolution cell imaging will be shown by means of FRET experiments exploiting the photochromic behavior of the acceptor to yield reliable estimate of resonance efficiency ("photochromic" FRET).

Materials and Methods

Protein Construction and Expression. The mammalian expression vector encoding for EQ1 was generated by site-directed mutagenesis of p-EGFP (Clontech version) using the primer E222Q: 5′-CACATGGTCCTGCTG-CAGTTCGTGACCGCCGCC-3′. The antisense primer had the respective reverse complementary sequence. To obtain the EYQ1 construct, we performed multiple rounds of point mutations (T65→S, T203→Y, and E222→Q) onto the sequence of EGFP cloned into *Hin*dIII-*Eco*RI sites of pcDNA3.1(+), by using the following primers: T65S: 5′-GTGACCACCCTGTCCTACGGCGTGCAG-3′; T203Y: 5′-CAACCACTACCTGAGCTACCAGTCCGCCCTGAG-3′; and E222Q (see above). The NLS-EYQ2 was generated by site-directed mutagenesis (T203→Y and E222→Q) starting from the construct NLS-EGFP described in ref 23. To obtain the construct EGFP-L_{20}-EYQ1 (p-EYQ1-EGFP), a first fragment was generated by PCR amplification of EYQ1 template and was inserted into *Hind*III-*Bam*HI sites of pcDNA3.1(+). The second EGFP was cloned by two steps of PCR amplification into *Bam*HI and *Xba*I sites, introducing a spacer linker of 20 amino acids (RGSASGGGGGLVPRG-SASGA) between the two EGFP sequences.

Recombinant Mut2Q was obtained as described in ref 24. The cDNA of EYQ1 was amplified by PCR and was cloned into *Bsa*I sites of p37plus IBA vector (IBA GmbH, Göttingen, Germany). Expression of recombinant EYQ1 protein was induced in log phase growing bacteria *Escherichia coli* BL21 DE3 strain (Invitrogen) upon treatment with anhydrotetracycline solution at 30 °C for 36 h.

Proteins fused to a 6xHistidine-tag were purified by affinity chromatography with a His-tag column (Sigma) following manufacturer instructions. The presence of a cleavage site for the Factor Xa protease between 6xHis-tag and the GFP sequence allowed the proteolytical removal of the histidine tag. A further anion exchange purification step and concentration of the proteins were carried out using a Millipore Centricon centrifugal filter units by using a buffer with 50 mM diethanolamine and 100 mM NaCl with the pH adjusted at 8.3 by adding HCl.

Absorption and Fluorescence Spectra. Absorption and fluorescence spectra were recorded at 23 °C on a Jasco V550 spectrophotometer (Jasco, Easton, MD) and a Cary Eclipse spectrofluorometer (Varian, Palo Alto, CA), respectively.

Extinction Coefficient and Quantum Yield Determination. The concentration of purified protein was determined from its absorption at 280 nm in the folded state using the extinction coefficient predicted from the protein sequence according to Pace's method[25] (a web-based calculation interface can be found at the

(9) Andresen, M.; Stiel, A. C.; Trowitzsch, S.; Weber, G.; Eggeling, C.; Wahl, M. C.; Hell, S. W.; Jakobs, S. *Proc. Natl. Acad. Sci. U.S.A.* **2007**, *104*, 13005–13009.
(10) Mizuno, H.; Mal, T. K.; Walchli, M.; Kikuchi, A.; Fukano, T.; Ando, R.; Jeyakanthan, J.; Taka, J.; Shiro, Y.; Ikura, M.; Miyawaki, A. *Proc. Natl. Acad. Sci. U.S.A.* **2008**, *105*, 9227–9232.
(11) Voliani, V.; Bizzarri, R.; Nifosi, R.; Abbruzzetti, S.; Grandi, E.; Viappiani, C.; Beltram, F. *J. Phys. Chem. B* **2008**, *112*, 10714–10722.
(12) Henderson, J. N.; Ai, H. W.; Campbell, R. E.; Remington, S. J. *Proc. Natl. Acad. Sci. U.S.A.* **2007**, *104*, 6672–6677.
(13) Dickson, R. M.; Cubitt, A. B.; Tsien, R. Y.; Moerner, W. E. *Nature* **1997**, *388*, 355–358.
(14) McAnaney, T. B.; Zeng, W.; Doe, C. F.; Bhanji, N.; Wakelin, S.; Pearson, D. S.; Abbyad, P.; Shi, X.; Boxer, S. G.; Bagshaw, C. R. *Biochemistry* **2005**, *44*, 5510–5524.
(15) Nifosi, R.; Ferrari, A.; Arcangeli, C.; Tozzini, V.; Pellegrini, V.; Beltram, F. *J. Phys. Chem. B* **2003**, *107*, 1679–1684.
(16) Kirber, M. T.; Chen, K.; Keaney, J. F., Jr. *Nat. Methods* **2007**, *4*, 767–768.
(17) Biteen, J. S.; Thompson, M. A.; Tselentis, N. K.; Bowman, G. R.; Shapiro, L.; Moerner, W. E. *Nat. Methods* **2008**, *5*, 947–949.
(18) Bizzarri, R.; Nifosi, R.; Abbruzzetti, S.; Rocchia, W.; Guidi, S.; Arosio, D.; Garau, G.; Campanini, B.; Grandi, E.; Ricci, F.; Viappiani, C.; Beltram, F. *Biochemistry* **2007**, *46*, 5494–5504.
(19) Brejc, K.; Sixma, T. K.; Kitts, P. A.; Kain, S. R.; Tsien, R. Y.; Ormo, M.; Remington, S. J. *Proc. Natl. Acad. Sci. U.S.A.* **1997**, *94*, 2306–2311.
(20) Yang, J. S.; Huang, G. J.; Liu, Y. H.; Peng, S. M. *Chem. Commun.* **2008**, 1344–1346.
(21) van Thor, J. J.; Gensch, T.; Hellingwerf, K. J.; Johnson, L. N. *Nat. Struct. Biol.* **2002**, *9*, 37–41.
(22) Patterson, G. H.; Lippincott-Schwartz, J. *Science* **2002**, *297*, 1873–1877.
(23) Cardarelli, F.; Serresi, M.; Bizzarri, R.; Giacca, M.; Beltram, F. *Mol. Ther.* **2007**, *15*, 1313–1322.
(24) Abbruzzetti, S.; Grandi, E.; Viappiani, C.; Bologna, S.; Campanini, B.; Raboni, S.; Bettati, S.; Mozzarelli, A. *J. Am. Chem. Soc.* **2005**, *127*, 626–635.
(25) Pace, C. N.; Vajdos, F.; Fee, L.; Grimsley, G.; Gray, T. *Protein Sci.* **1995**, *4*, 2411–2423.

ExPASy Proteomics Server, http://www.expasy.ch/tools/protparam-.html). Notably, the accuracy of the predicted extinction coefficients was checked by the denaturation method of Edeloch.[26] The degree of chromophore maturation was calculated from the protein concentration by Ward's method, which requires protein denaturation in 0.2 M NaOH and absorption read-out at 448 nm: assuming 100% maturation, $\varepsilon_{448} = 33\,500\ M^{-1}\ cm^{-1}$.[27,28] Protein quantum yields were determined by using fluorescein as standard ($\Phi_{Fluo} = 0.92$ in 0.1 M NaOH). More in detail, the absorption and fluorescence emission spectra ($\lambda_{ex} = 476$ nm) of a protein solution (pH = 8.2, 20 mM DEA) and fluorescein (0.1 M NaOH) were collected sequentially; the absorption of both samples was kept below 0.08 to avoid inner filter effects. The protein quantum yield was calculated by the equation

$$\Phi_P = \Phi_{Fluo}\frac{F_P}{A_P}\frac{A_{Fluo}}{F_{Fluo}}\frac{n_P^2}{n_{Fluo}^2} \quad (1)$$

where F_P and F_{Fluo} are the integrated fluorescence intensities from 480 to 700 nm, A_P and A_{Fluo} are the absorbances at 476 nm, and n_P and n_{Fluo} are the refraction indexes of protein and fluorescein solutions, respectively (we took them equal to 1.33).

Protein Irradiation in Solution. Proteins were dissolved in buffers (2 mM citrate/10 mM phosphate or 10 mM MOPS) at selected pH in 1 cm path quartz cuvettes (Hellma, Müllheim, Germany) supplied with a magnetic stirrer. Under stirring, the protein solution was front-face irradiated for selected times by using continuous wave laser light (405 nm: FP-40/7AF-AV-SD5 laser, Optoprim, Monza, Italy; 476 and 514 nm: Stabilite 2017 ion laser, Spectra-Physics, Mountain View, CA). The power of the laser beam exiting from the solution was monitored over time by a Power/Energy Meter 841-PE (Coherent Italia, Milano, Italy).

Stopped-Flow/pH-Jump Experiments. Stopped-flow experiments were carried out in a Olis RSM 1000 (Olis, Bogart, GA) spectrophotometer/spectrofluorometer apparatus equipped with a RX 2000 rapid mixing accessory (Applied Photophysics, Leatherhead, UK). Experimentally measured dead time of RX 2000 was 35 ms. Protein solution at pH 7.2−7.6 was irradiated in 1 cm path quartz cuvettes until significant photoconversion was achieved. Then, the solution was transferred in the RX 2000, whose cuvette was placed inside the RSM 1000. The pH of the protein solution was increased by fast mixing with a 20 mM diethanolamine buffer at pH 10 in the stopped-flow apparatus, and absorption or fluorescence spectra were collected by the RSM 1000 immediately afterward. The final pH of the solution was measured after the optical measurement.

Cell Culture and Transfections. HeLa cells (CCL-2 ATCC) were grown in Dulbecco Modified Medium (DMEM) supplemented with fetal bovine serum (10%) with glutamine (2 mM), penicillin (10 U/mL), and streptomycin (10 μg/mL) at 37 °C and in 5% CO_2 atmosphere. CHO K1 cells (CCL-61 ATCC) were grown in Ham's F12K medium supplemented with 10% fetal bovine serum at 37 °C and in 5% CO_2. Transfections were carried out by using lipofectamine reagent (Invitrogen) according to the manufacturer's instructions. For live imaging, 10×10^4 cells were plated 24 h before transfection onto a 35 mm glass bottom dish (WillCo-dish GWSt-3522). Due to the slower maturation kinetics of E222Q proteins,[29] cells were imaged 36−48 h after transfection.

Cell Imaging. Cell fluorescence was measured using a Leica TCS SP2 inverted confocal microscope (Leica Microsystems AG, Wetzlar, Germany). Glass bottom Petri dishes containing transfected cells were mounted in a thermostatted chamber (Leica Microsystems) and imaged by a 40× 1.25 NA oil immersion objective (Leica Microsystems). The 476 and 514 nm excitation sources were provided by the in-line Ar laser of the microscope; the 403 nm excitation source was provided by an external laser pulsing at 1 MHz (Hamamatsu Photonics Italia, Milan, Italy). The average intensity at the focus point of the objective was calculated according to ref 8. Fluorescence was detected by AOBS-based built-in detectors of the confocal microscope. In scan mode, line speed was set to 1000 Hz and pixel size to 256 × 256; the pixel dwell time was approximately 1.2 μs. Each image was the average of two frames and was acquired every 0.78 s. Zooms were in the 4−7 range. Imaging data were analyzed by Leica Imaging package version 2.61 and ImageJ software (NIH Image, http://rsb.info.nih.gov/nih-image/index.html).

Results

General Photochromic Properties. The first two mutants investigated here are Mut2Q (S65A/V68L/S72A/E222Q GFP) and EYQ1 (F64L/T203Y/E222Q GFP). Mut2Q is a green-emitting protein whose absorption ($\lambda = 496$ nm, $\varepsilon = 54\,000\ M^{-1}\ cm^{-1}$) and fluorescence ($\lambda = 507$ nm, $\Phi = 0.28$) at physiological pH can be attributed solely to the anionic (B) state of the chromophore (Figure 1a). In fact, the p*K* of Mut2Q was found to be around 6.0.[24] The B state of EYQ1, conversely, is yellow-emitting ($\lambda = 524$ nm, $\Phi = 0.72$), and its absorption spectrum displays, beside the B peak ($\lambda = 510$ nm, $\varepsilon = 73\,000\ M^{-1}\ cm^{-1}$), some residual contribution from the neutral chromophore (A state, $\lambda = 411$ nm, $\varepsilon = 27\,900\ M^{-1}\ cm^{-1}$, almost nonfluorescent) at physiological pH (Figure 1b). For EYQ1, we measured p$K = 6.87$.

In spite of the different optical properties, illumination near the maximum wavelength of the B state leads to the same modification of absorption: the anionic band decreases in intensity, whereas a blue-shifted nonfluorescent state (A_t; we denote it A_t for reasons that will be clear in the following) emerges (Mut2Q: $\lambda = 403$ nm, EYQ1: $\lambda = 413$ nm, Figure 1c,d). Irradiation of A_t restores fluorescence and B state for both proteins (Figure 1c,d). A photostationary condition, for which the on- and off-switching rates compensate each other, is eventually reached at any illumination wavelength within the absorption range of the B band. As the switching rate is linearly proportional to the number of absorbed photons (Supporting Information), the fraction of photoswitched protein depends on the overlap of B and A_t absorption bands.[11] This explains why reactivation of Mut2Q at 405 nm leads to a photostationary state where the A_t state does not disappear (Figure 1c). Alternate excitation at B and A_t maxima affords fluorescence cycling in vitro (protein in solution or immobilized in a polyacrylamide gel[30]) or in vivo with minor loss of absorption or emission (<3% per cycle, Figure 2d,e and Figure S1a in Supporting Information).

We also tested the effect of E222Q replacement in the green variant EGFP (F64L/S65T GFP) and the yellow variant E^{2}GFP (F64L/S65T/T203Y GFP). These mutants were only expressed in cells. The optical properties of EQ1 (E222Q EGFP) are analogous to those of EGFP;[27] those of EYQ2 (E222Q E^{2}GFP) were found to be similar to EYQ1. Remarkably, we found that cell-expressed EQ1 and EYQ2 are characterized by the same photochromic behavior of Mut2Q and EYQ1, respectively (Figure 2). Thus, E222Q bestows efficient photochromicity on four photostable AFPs differing for the original mutation pattern and spectroscopic properties. Note that our mutants are quite stable at ambient light, in spite of the low-intensity photoswitching.

(26) Gill, S. C.; von Hippel, P. H. *Anal. Biochem.* **1989**, *182*, 319–326.
(27) Sniegowski, J. A.; Lappe, J. W.; Patel, H. N.; Huffman, H. A.; Wachter, R. M. *J. Biol. Chem.* **2005**, *280*, 26248–26255.
(28) Sniegowski, J. A.; Phail, M. E.; Wachter, R. M. *Biochem. Biophys. Res. Commun.* **2005**, *332*, 657–663.
(29) Pouwels, L. J.; Zhang, L.; Chan, N. H.; Dorrestein, P. C.; Wachter, R. M. *Biochemistry* **2008**, *47*, 10111–10122.
(30) Di Benedetto, F.; Biasco, A.; Bizzarri, R.; Arosio, D.; Ricci, F.; Beltram, F.; Cingolani, R.; Pisignano, D. *Langmuir* **2006**, *22*, 29–31.

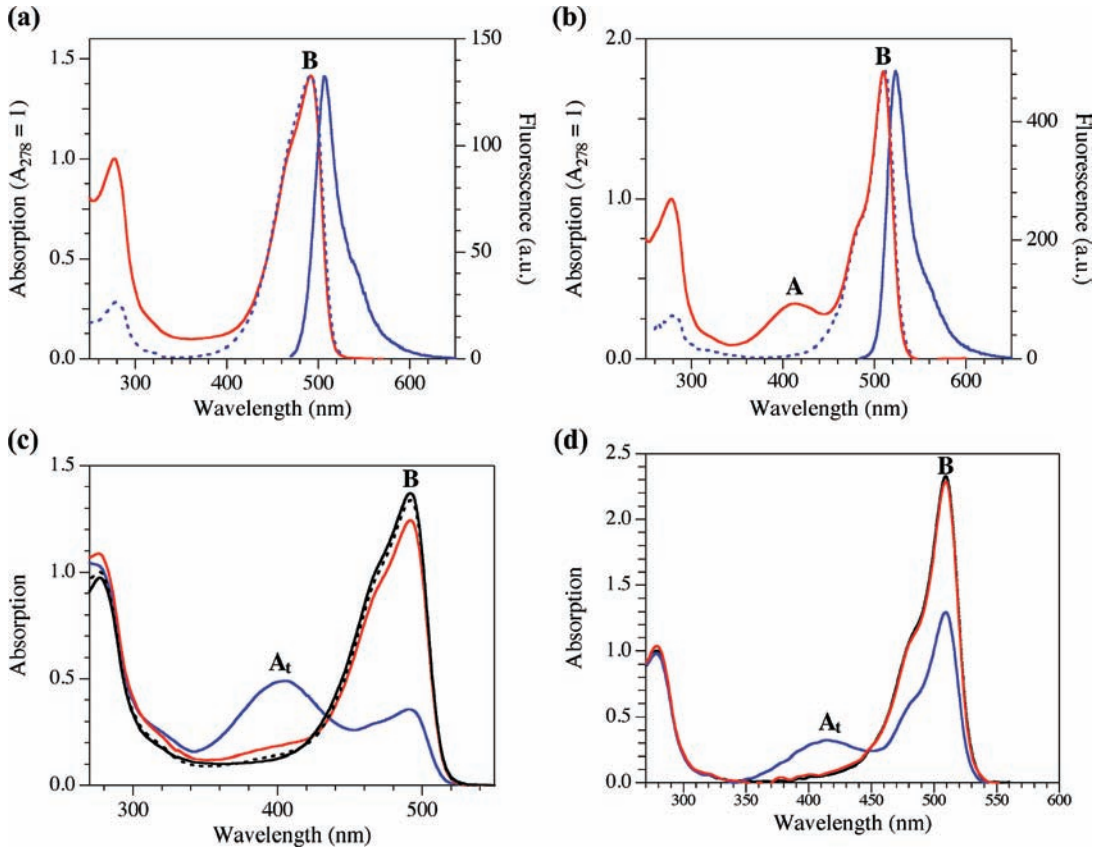

Figure 1. Absorption, emission, and excitation of Mut2Q (a) and EYQ1 (b) at pH 7.2; A and B states are indicated. (c) Photochromic cycle of Mut2Q followed by absorption. The native protein (pH 7.4, black line) was at first illuminated at 476 nm (0.5 W/cm^2, 4′) to populate the dark A_t state (blue line). Then, the protein was illuminated at 405 nm (0.06 W/cm^2, 2′), repopulating the anionic fluorescent B state (red line). Finally, the protein was allowed to relax thermally for 2 h (dotted black line). (d) Photochromic cycle of EYQ1 followed by absorption. The native protein (pH 8.7, black line) was at first illuminated at 514 nm (0.5 W/cm^2, 4′) to populate the dark A_t state (blue line). Then, the protein was illuminated at 405 nm (0.06 W/cm^2, 1′), repopulating the anionic fluorescent B state (red line); note that almost no final thermal relaxation was required to restore the initial conditions on account of the optical separation between the A_t and B states.

Spontaneous Recovery and Protonation Reaction of *trans* State. Isolated AFP chromophores and many photochromic FPs display spontaneous (thermal) return from the dark state to the bright state.[11,31] Thus, we set out to verify whether such as property is shared also by our E222Q mutants. In our procedure, Mut2Q and EYQ1 were initially photoconverted to A_t and then maintained in the dark at constant temperature while their absorption spectra were monitored over time. Noticeably, we found that both Mut2Q and EYQ1 show a complete spontaneous recovery from A_t to B (Figure 3a). This recovery follows a strict first-order (i.e., monoexponential) kinetics whose amplitude and time constant depends on the solution pH (Figure 3b,c). At neutral pH (pH was kept above 7 to ensure a significant B population), the spontaneous recovery is slow (few hours), whereas at very high pH, the B state is restored in a few seconds. Above pH 10.5, however, significant protein unfolding prevented further kinetic measurements.

Next, we carried out experiments to understand better the origin of pH modulation of the thermal recovery rate from the dark to bright state in Mut2Q and EYQ1. A suggestive hypothesis, already proposed for mTFP mutants from *Clavularia*[12] and Dronpa,[9] takes into account the ionization of the chromophore in the *trans* state. In such a case, different energy barriers between *trans* and *cis* configurations must exist for the protonated and anionic chromophore states. This hypothesis is supported by theoretical calculations[32] and data on isolated chromphores.[33] An alternative explanation considers the conformational rearrangement of a nearby ionizable residue (e.g., His^{148} or Arg^{96}) upon protonation/deprotonation, which in turn would sterically lock/unlock the *trans* chromophore. To discriminate between these two hypotheses, we carried out photoconversion/pH-jump experiments with both EYQ1 and Mut2Q. First, the protein was photoswitched to the dark state near neutral pH (Figure 3d, black and red traces). The slow spontaneous recovery of A_t to B at this pH allowed the transfer of the photoconverted solution in a stopped-flow apparatus. Here, the pH was suddenly increased by fast mixing with a basic buffer, and the absorption spectrum of the protein was collected shortly (40 ms) afterward. Remarkably, A_t band was mostly converted to a new band similar to that of anionic B state (Figure 3d, green trace). This band was found to evolve to the actual B band with the expected time constant for thermal recovery at the set final pH (Figure 3d, blue trace). These findings suggest that the *trans* chromophore is characterized by a protonation equilibrium, most likely at its phenolic group.

Under this assumption, the recovery rate versus pH plot allows for the calculation of pK_t, that is, the pK_a of the *trans*

(31) Stiel, A. C.; Trowitzsch, S.; Weber, G.; Andresen, M.; Eggeling, C.; Hell, S. W.; Jakobs, S.; Wahl, M. C. *Biochem. J.* **2007**, *402*, 35–42.
(32) Voityuk, A. A.; Michel-Beyerle, M. E.; Rosch, N. *Chem. Phys. Lett.* **1998**, *296*, 269–276.
(33) He, X.; Bell, A. F.; Tonge, P. J. *FEBS Lett.* **2003**, *549*, 35–38.

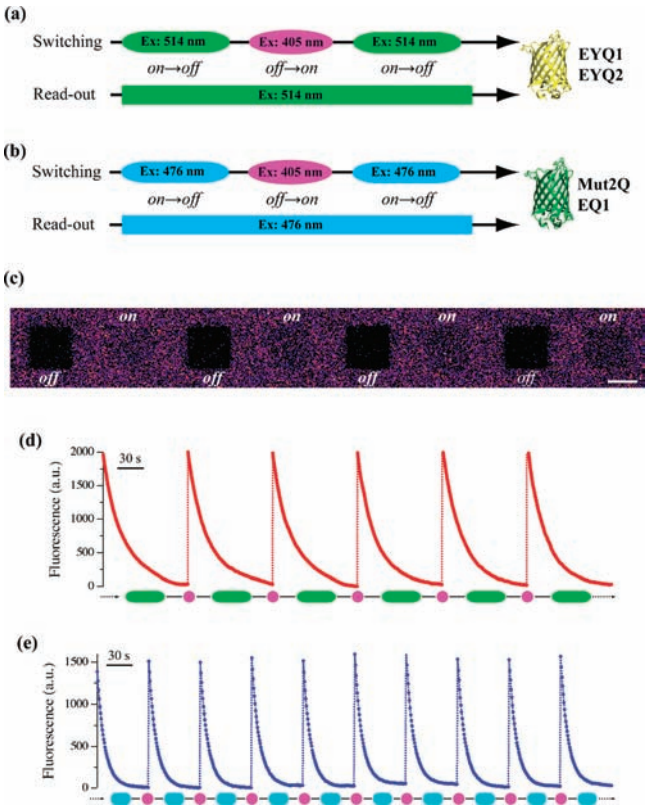

Figure 2. (a) Photoswitching scheme of yellow photochromic mutants EYQ1 and EYQ2. Switching was carried out by alternating 514 and 403 (or 405) nm excitation; fluorescence read-out was provided by continuous 514 nm excitation. Note that illumination at 514 nm was tuned to obtain concomitant switching off and fluorescence read-out. (b) Photoswitching scheme of green photochromic mutants Mut2Q and EQ1. Switching and read-out were carried out as for EYQ1 and EYQ2, but 514 nm excitation was replaced by 476 nm excitation. (c) Photoswitching of EYQ1 immobilized in a polyacrylamide gel at pH 7.8 imaged by confocal microscopy A 13.1 μm × 13.1 μm was photoswitched according to the scheme of panel (a). Light intensities at focal plane were 0.8 kW/cm^2 for 514 nm and 0.06 kW/cm^2 for 405 nm. Scale bar = 5 μm. (d,e) Fluorescence emission during photoswitching cycles in HeLa cells imaged by confocal microscopy. EYQ1 (d) or EQ1 (e) was photoswitched according to the scheme of panel (a) or (b), respectively. At the bottom of the two plots, the alternating sequence of 514/476 and 403 nm illumination is pictorially represented by green/cyan and violet ellipses. Light intensities at focal plane were 20−50 kW/cm^2 for 476/514 nm and 2 kW/cm^2 for 403 nm.

chromophore. Indeed, thermal recovery data can be fitted to the sigmoidal equation that is associated with a single protonation equilibrium.[18] Although the data do not extend to very high pH values preventing the visualization of the leveling off of the sigmoidal curve, data fitting yielded pK_t with good accuracy for both proteins. We found pK_t (Mut2Q) = 9.38 ± 0.07 and pK_t (EYQ1) = 9.87 ± 0.08. Notably, these values are about 3 pH units higher than the corresponding pK in the *cis* form. Also, Mut2Q displays a faster thermal recovery from the *trans* state for both protonated and anionic chromophore forms compared to EYQ1.

Nature of the Dark State(s). Our group recently demonstrated by Raman analysis that A_t of EYQ1 corresponds to the *neutral trans form* of the chromophore (hence the symbol A_t).[34] This explains why A_t has an absorption spectrum similar to the neutral state of the native protein and implies that a *cis*↔*trans* photoisomerization mechanism is the basis of the observed protein photochromism, likewise isolated AFP chromophores.[11,34] On the basis of these results, we can propose a photophysical model that successfully rationalizes all experimental findings on E222Q proteins (Scheme 1): (1) a reversible *cis*↔*trans* photoisomerization is responsible for the optical switching (Scheme 1, open arrows with bolts); (2) both the *cis* and *trans* isomers participate to a fast (<ms) protonation equilibrium with the external buffer (Scheme 1, equilibrium arrows); (3) each *trans* state can thermally relax to its *cis* counterpart (Scheme 1, curved single arrows), although the energy barrier depends on the protonation state of the chromophore (fast if anionic, very slow otherwise).[32,35] Note that in Scheme 1 we do not specify the initial and final state of the reversible photoisomerization. Indeed, excitation of any ground state can in principle lead, through an internal conversion pathway, to another ground state with different stereochemistry change. The protonation of the final state, however, is not necessarily the same as that of the initial one, as a concerted isomerization−protonation(deprotonation) mechanism could take place. We are currently carrying out experiments in order to check this possibility. Regardless of internal conversion mechanism, our model explains why the photoisomerization of the native (*cis*) protein at pH 7−9 leads to the preferential formation of the *trans* neutral state A_t. Instead, photoisomerization at pH > 9.5/10 leads to the *trans* anionic state B_t similar to B, as confirmed by the small spectral change obtained at these pH values (not shown).

Absorption and Emission Spectra of *trans* Forms. Following our photophysical model of photochromism, the absorption spectra of Mut2Q and EYQ1 *trans* (A and B) states can be determined from pH-jump data and *cis* spectra starting from the following considerations: (1) loss of B population upon initial illumination is paralleled by an equivalent enrichment of A_t; (2) the pH jump only transfers population between A_t and B_t. More in detail, the following steps led to spectral deconvolution:

• The switched *off* spectrum at neutral pH (Figure 3d, red line) contains a mixture of A_t, A, and B, whereas the spectrum before the photoconversion (Figure 3d, black line) contains only A and B. Let us denote the former as PC and the second as NC. Note that in both PC and NC the A/B ratio is the same since the pH is unchanged and the proton equilibrium is consequently not modified.

• NC was scaled to have the bands at $\lambda > 510$ nm in register with that of PC; at these wavelengths, only B absorbs appreciably, and this operation ensured that both spectra were characterized by the same B absorbance. This implied that also A absorbance was the same in both PC and scaled NC, owing to the aforementioned constancy of the A/B ratio. Note that the scaling factor represents the molar fraction of non photoconverted protein.

• Subtraction of scaled NC from PC yielded a spectrum containing only A_t. The pure A_t spectrum was obtained by dividing this difference spectrum by the fraction of photoconverted proteins (i.e., 1-scaling factor).

• The postjump spectrum (Figure 3d, green line) contains a mixture of B_t, A_t, and B (A is not stable at very high pH). Let us denote it as PJ. To recover the pure B_t spectrum, we first subtracted from PJ the A_t spectrum scaled as to put in register the bands at $\lambda < 415$ nm. This operation allowed the complete

(34) Luin, S.; Voliani, V.; Lanza, G.; Bizzarri, R.; Amat, P.; Tozzini, V.; Serresi, M.; Beltram, F. *J. Am. Chem. Soc.* **2009**, *131*, 96–103.

(35) Weber, W.; Helms, V.; McCammon, J. A.; Langhoff, P. W. *Proc. Natl. Acad. Sci. U.S.A.* **1999**, *96*, 6177–6182.

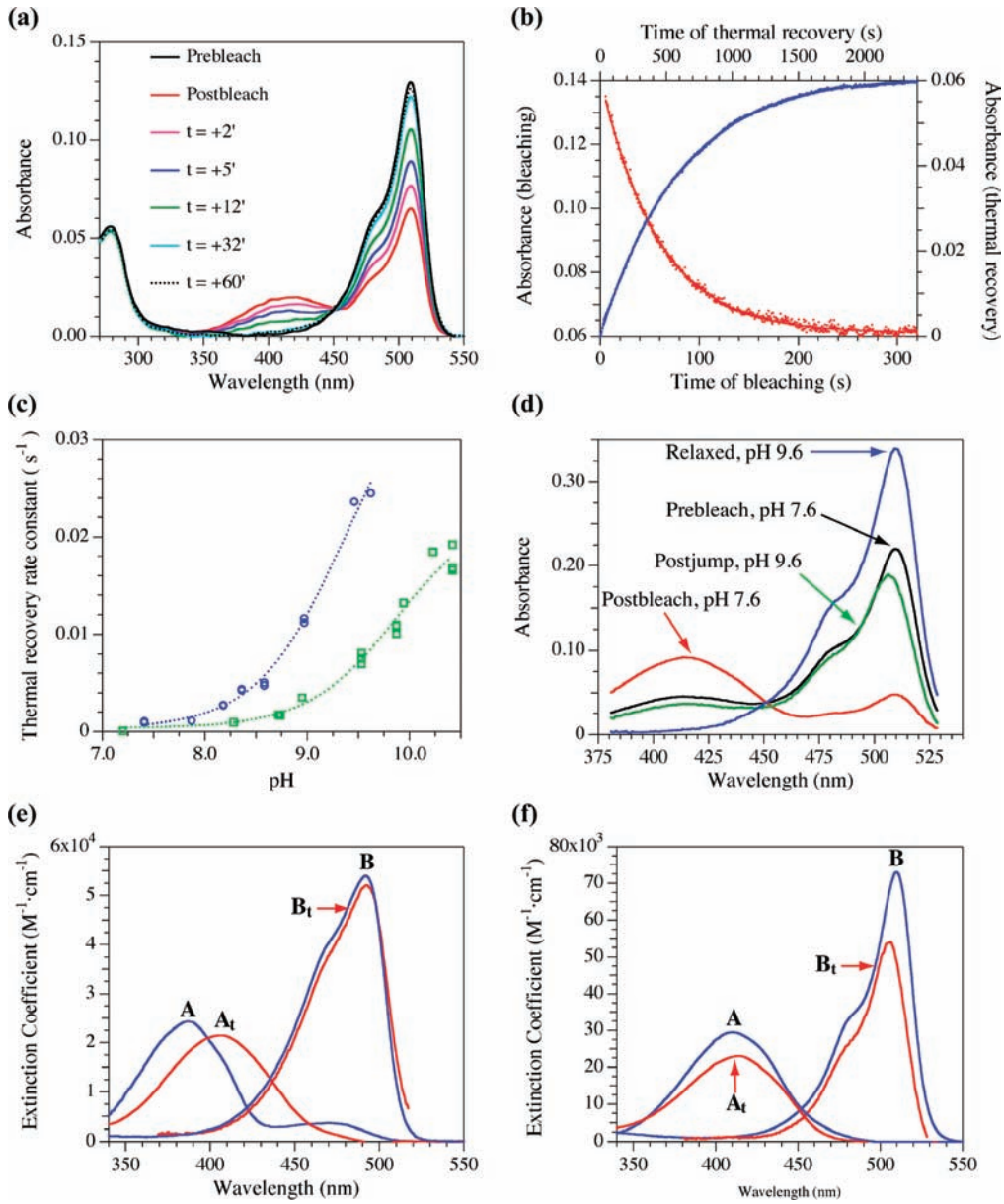

Figure 3. (a,b) On→off photoswitching (0.5 W/cm^2) and subsequent thermal recovery from the dark state for EYQ1 at pH 8.74 and $T = 25$ °C. The on- and off-absorption spectra, as well as those collected at different times during thermal recovery, are reported in panel (a). The time evolution of absorbance at 514 nm during the on→off photoswitching (red dots) and thermal recovery (blue dots) are reported in panel (b). Following our kinetic model of photoconversion (Supporting Information), the on→off photoswitching trace is fitted to eqs 12−14 (red line); instead, the recovery trace is fitted to a monoexponential curve (blue line). (c) Dependence of the first-order rate constant of thermal recovery upon pH for Mut2Q (blue trace) and EYQ1 (green trace). The curves were fitted to the binding equation typical of single proton ionization, finding Mut2Q (p$K_t = 9.38 \pm 0.07$) and EYQ1 (p$K_t = 9.87 \pm 0.08$), where pK_t is the pH at half amplitude. (d) A pH-jump experiment on EYQ1 after photoconversion; for description see text. (e,f) Molar absorption spectra of the four ground states (*cis* forms, blue traces; *trans* forms, red traces), which are accessible to Mut2Q (e) and EYQ1 (f). The *trans* spectra were deconvolved starting from the spectra collected in the pH-jump experiment (see text for details).

removal of the A_t absorbance from PJ. Then, we subtracted also the B spectrum scaled by the fraction of nonphotoconverted protein (indeed, the full nonphotoconverted population must be in B state since the pH jump led to complete transfer of A population into B). The double subtraction yielded a difference spectrum reflecting only B_t. Pure B_t was obtained by normalization of the difference spectrum by the molar fraction of B_t, calculated from the pK_t value of the protein and the pH after the jump.

Figure 3e,f displays the absorption spectra of the four forms of EYQ1 and Mut2Q, respectively. The comparison of the absorption properties of the *cis* and *trans* isomers in different protonation states indicates that (i) A_t is slightly red-shifted compared to A, (ii) B_t is slightly blue-shifted compared to B, and (iii) *trans* forms have lower molar absorption compared to *cis* ones. The same scheme of pH-jump experiment was used by monitoring protein fluorescence and allowed us to determine the emission and quantum yield of state B_t for both proteins. We found that B_t has approximately the same emission spectrum and quantum yield of B (for EYQ1: $\Phi_{Bt} = 0.70$, for Mut2Q: $\Phi_{Bt} = 0.21$).

Photoconversion Quantum Yields. The inverse of the number of absorbed photons per *cis*→*trans* or *trans*→*cis* photoconversion event is called photoswitching yield (φ) and expresses the

Scheme 1. Photophysical Scheme Describing the Reactive Processes Connecting the Four Ground States Accessible to the Chromophore of E222Q Proteins[a]

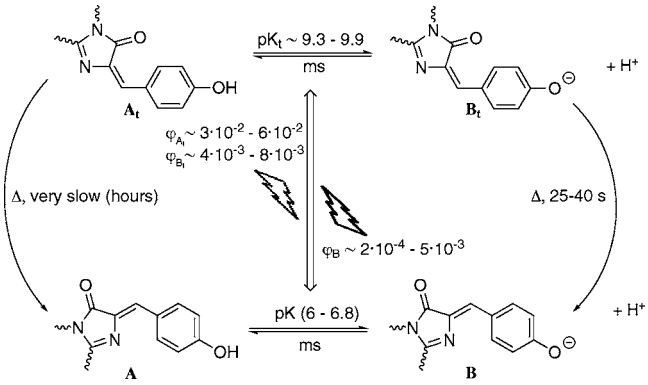

[a] A,B represent the *cis* neutral and anionic forms, respectively; A_t and B_t represent the *trans* neutral and anionic forms, respectively. Note that state A_t corresponds to the generic dark state, which is obtained by reversible photoswitching of B at pH near neutrality. The open double arrow refers to the reversible photoisomerization process; the single arrows refer to the thermal decay from *trans* states to *cis* states; the equilibrium arrows refer to the protonation reaction in either the *cis* or *trans* forms; estimate of the intrinsic photoswitching yields, the time constants of thermal recovery, and p*K* values are also reported.

intrinsic efficiency of the isomerization process.[36] This parameter was determined for both Mut2Q and EYQ1 as follows. To this end, in a cuvette, we performed steady-state and pulsed-excitation experiments that showed linear dependence between excitation intensity and off-/on-switching rates. These findings are in excellent agreement with what we previously determined for isolated AFP chromophores.[11] Then, protein solutions at given pH (pH range 7.2−10.2) and temperature values were laser-illuminated in the B band range (514 and 476 nm for EYQ1, 476 nm for Mut2Q), while absorbance at the same wavelength was being recorded (Figure 3b). The time-dependent absorption decays were fitted to a kinetic scheme similar to that developed for the one-photon photoconversion of isolated AFP chromophores but now integrated with the protonation equilibria of both *cis* and *trans* isomers (Supporting Information). Our kinetic treatment introduces effective photoswitching yields φ_{off} and φ_{on} that take into account the actual isomer population and are hence directly *measurable* at a given certain wavelength. In more detail, φ_{off} and φ_{on} are derived from the intrinsic φ's by the optical properties and relative population (and hence the experiment pH value) of neutral and anionic states for both the *cis* and *trans* isomers.

Data analysis gave pH-independent φ_{off} values for Mut2Q and EYQ1 (Table 1). Indeed, only state B is addressed by illumination in both proteins at these wavelengths and pH > 7.2, and we can therefore identify the measured effective yields to the intrinsic φ_B values (Table 1). Data indicate that Mut2Q *cis*→*trans* photoisomerization processes are more than 1 order of magnitude faster than EYQ1. On the contrary, experimental φ_{on} values depend on buffer pH, as expected owing to the possible presence of one or both *trans* isomers at pH between 7.2 and 9.8. Fitting φ_{on} data (for EYQ1 also at 476 nm) to eq 11 (Supporting Information) yielded estimates of the *trans*→*cis* photoswitching yields for both A_t and B_t (φ_{A_t} and φ_{B_t}, respectively, Table 1).

It can be noted that *trans*→*cis* photoswitching yields are 1−2 orders of magnitude higher than their *cis*→*trans* counterparts. Also, φ_{A_t} is about 1 order of magnitude higher that φ_{B_t} for both mutants. Remarkably, similar values and trends were reported for Dronpa[8] and its derivatives,[31] whereas they are 2−3 orders of magnitude larger than those found for the known photochromic AFPs (Table 1). We should note, however, that these switching yields are still lower than those measured for the AFP chromophore, arguably because of a residual hampering effect of the surrounding residues on the photoisomerization process.[11]

Estimate of the Quantum Yield of Irreversible Photobleaching. Our kinetic calculation of photoconversion quantum yields is valid for a system where the irreversible photobleaching of the protein is negligible, and the overall concentration of "active" protein (*cis*+*trans*) is not significantly affected. Indeed, we found that only a minor fraction of the protein is photodestructed in one of the *on*−*off* photoconversion cycles that we considered for calculation (≤3%). The quantum yield of irreversible photobleaching φ_{irr}, however, is a very important parameter because this limits the eventual signal-to-noise of any imaging method and the ability to localize single molecules. A good estimate of this parameter can be obtained by a simple kinetic reasoning that takes into account the ratio between the fraction of irreversibly photobleached proteins after one *on*→*off* switching and the number of absorbed photons by the bright state (Supporting Information). By this method, we found φ_{irr} around 10^{-5} (Table 1), in excellent agreement with previously measures of this parameter in GFPs.[37] It is worth noting that our estimate attributes this yield to the bright B state. Although it is possible that partial photodestruction takes place also from the A_t dark state, the interest is usually devoted to the stability of the bright state of the protein, whose φ_{irr} should accordingly represent the highest limit. Also, we showed that the *on*→*off* (i.e., B→A_t) conversion requires more photons (and therefore is slower) than the *off*→*on* (i.e., A_t→B) conversion; we may reason that the phenomena that lead to chromophore degradation are more likely to occur during the longer *on*→*off* time than the shorter *off*→*on* time.

Photochromic FRET Applications. Photochromic fluorescent probes were proposed as acceptors to overcome most of the major artifacts and limitations affecting conventional FRET methods by means of repeated acceptor photobleaching cycles ("photochromic FRET").[38] Yellow EYQ1 and EYQ2 are excellent candidates for this new FRET methodology owing to their red-shifted absorption spectra which make them excellent acceptors in tandem with cyan and green (A)FP donors. The possibility of measuring FRET between green and yellow variants is particularly attractive since the extended spectral overlap between donor emission and acceptor absorption determines a large Förster radius (R_0 = 5.64 nm for the GFP−YFP couple[39]). In order to assess the suitability of the present mutants for FRET measurements, we produced the construct EGFP-L_{20}-EYQ1, where L_{20} is a 20 amino acid long flexible linker,[40] and we imaged it in vivo by confocal microscopy.

(36) Sinnecker, D.; Voigt, P.; Hellwig, N.; Schaefer, M. *Biochemistry* **2005**, *44*, 7085–7094.
(37) Harms, G. S.; Cognet, L.; Lommerse, P. H.; Blab, G. A.; Schmidt, T. *Biophys. J.* **2001**, *80*, 2396–2408.
(38) Jares-Erijman, E. A.; Jovin, T. M. *Nat. Biotechnol.* **2003**, *21*, 1387–1395.
(39) Patterson, G. H.; Piston, D. W.; Barisas, B. G. *Anal. Biochem.* **2000**, *284*, 438–440.

Table 1. Intrinsic Photoswitching and Irreversible Photobleaching Yields (Absorbed Photons^{-1}) for Mut2Q and EYQ1[a]

protein	φ_B	φ_{A_t}	φ_{B_t}	φ_{irr}
Mut2Q (S65A/V68L/S72A/E222Q GFP)	$(4.7 \pm 2.5) \times 10^{-3}$	$(2.6 \pm 0.6) \times 10^{-2}$	$(8.0 \pm 3.0) \times 10^{-3}$	$(5 \pm 3) \times 10^{-5}$
EYQ1 (F64L/T203Y/E222Q GFP)	$(1.8 \pm 0.5) \times 10^{-4}$	$(6.0 \pm 1.0) \times 10^{-2}$	$(4.0 \pm 1.0) \times 10^{-3}$	$(1.9 \pm 0.1) \times 10^{-5}$
YFP (S65G/S72A/T203Y GFP)[13,37]	$\sim 10^{-6}$	$\sim 10^{-5}$ [b]	*nd*	5.5×10^{-5}
E^{2}GFP (F64L/S65T/T203Y GFP)[15]	1.1×10^{-7}	*nd*	1×10^{-6}	*nd*
Dronpa[8]	3.2×10^{-4}	3.7×10^{-1}	*nd*	*nd*
synthetic GFP chromophore[11,20]	2.0×10^{-1} (*cis*→*trans*)		2.0×10^{-1} (*trans*→*cis*)	*nd*

[a] Data for other FPs are reported for comparison (in italic); φ_B refers to the *cis*→*trans* photoisomerization from state B; φ_{A_t} and φ_{B_t} refer to the *trans*→*cis* photoisomerization from states A_t and B_t, respectively (Scheme 1); φ_{irr} is the quantum yield for irreversible photobleaching from state B. [b] Estimated from single molecule switching-on data reported in ref 10, assuming $\varepsilon(A_t) \sim \varepsilon(A) \sim 25\,000\ M^{-1}\ cm^{-1}$.

The theoretical treatment of FRET emission in the presence of a photochromic acceptor such as the present AFPs (see Supporting Information) shows that, upon acceptor bleaching or reactivation, a linear relation must hold between the fluorescence emission collected in two separate spectral ranges (in our notation, $F^{(1)}$ and $F^{(2)}$). On the basis of EGFP and EYQ1 photophysics, we selected two spectral regions ($F^{(1)}$, 485−500 nm; $F^{(2)}$, 509−525 nm) for which the functional relationship between the $F^{(1)}$ versus $F^{(2)}$ slope and the FRET efficiency E is particularly simple (see Supporting Information). As expected, the partial switching off of EYQ1 leads to the increase of EGFP fluorescence, detected in the $F^{(1)}$ interval (Figure 3a,b). Reactivation of EYQ1 restores the original fluorescence signal (Figure 4a,b). Notably, the excitation wavelength (476 nm) allowed both cell imaging and photoconversion of the photochromic acceptor protein.

$F^{(1)}$ versus $F^{(2)}$ fluorescence plots display a linear trend (Figure 4c). Minor deviations from linearity were sometimes detected because of slight cell defocusing. Note that significant irreversible photobleaching of the donor and/or the acceptor, both from direct excitation and forward/reverse energy transfer, would change the $F^{(1)}$ versus $F^{(2)}$ slope at each cycle, owing to the change in the stoichiometric ratio between "emissive" donor and acceptor (Supporting Information). In the present case, however, we carried out measurements on AFP mutants whose irreversible photobleaching is negligible for a few photoswitching cycles (in typical conditions, >91% of EYQ1 are still active after three cycles).

Linear fitting of $F^{(1)}$ versus $F^{(2)}$ fluorescence yielded $E = 32 \pm 4\%$ (41 cells). Note that this E value must be considered as the net result of two FRET processes (effective FRET efficiency; see Supporting Information). In fact, the extended spectral overlap allows also reverse FRET between EYQ1 (now the donor) and EGFP (now the acceptor) to occur when fluorescence is excited at 476 nm (see Supporting Information). From the known distance between the protein chromophores,[40] and the Förster radii calculated for both the direct and reverse FRET, we estimate $E = 35\%$, in agreement with the experimental data. We should like to stress that the EGFP-L_{20}-EYQ1 construct can be used as a standard for in vivo FRET measurements involving EGFP and EYQ1 (see Supporting Information).

Discussion

Mutation E222Q was investigated in a few AFP mutants before this work, and a strong influence on the photophysical properties of the chromophore was always reported. The most evident effect of E222Q is the thermodynamic stabilization of the anionic form of the chromophore brought by its impact on proton-exchange pathways of protein H-bond networks.[18,24,29] This effect is paralleled by the modification of the excited-state proton-transfer mechanism (ESPT), which is responsible for the emission properties of the neutral state and involves E222 as final acceptor in most AFPs.[18,19] Finally, FCS measurements showed that E222Q AFPs exhibit a pH-independent fluorescence flickering characterized by an intensity- and wavelength-dependent dark-state fraction, a property that led several authors to suggest the presence of reversible photoconversion channels.[41−44] These results prompted us to investigate the effect of the E222Q replacement on the photochromic properties of AFPs. We found that E222Q induced efficient reversible photoswitching in four distinct AFP mutants and therefore may represent a general promoter of AFP photochromism.

Our spectroscopic studies on the green mutant Mut2Q (S65A/V68L/S72A/E222Q GFP) and the yellow mutant EYQ1 (F64L/T203Y/E222Q) afforded a clear picture of the photophysical mechanisms underlying E222Q AFP photochromism that is shown in Scheme 1. The native stereochemistry of the protein chromophore is *cis* with respect to its internal double bond (Scheme 1).[34] Changing the pH of the solution represents a first way to modify protein optical properties because this promotes the reversible conversion between the neutral state (A, nonfluorescent, absorption peaked around 400 nm) and the anionic state (B, fluorescent, absorption peaked around $\lambda = 496$ nm for Mut2Q and $\lambda = 514$ for EYQ1) of the chromophore. The pK value of this reaction is typically between 6 and 6.9, and therefore at pH > 7, the anionic chromophore is the predominant form (Figure 1a,b). The optical properties of the native proteins can also be changed by photoexcitation that can lead to photoisomerization of the AFP chromophore from a *cis* to a *trans* configuration (Scheme 1).[34] Also, this process is reversible and allows for repeated switching between optical states with different characteristics (Figure 1c,d). This reversible switching was also shown here for two additional E222Q mutants (EQ1 and EYQ2) in living cells (Figure 2).

After the *trans*→*cis* photoisomerization, *trans* chromophores can revert thermally back to their *cis* configuration following a first-order kinetics (Figure 3a,b). This phenomenon was observed in other photochromic FPs and derives from the higher energy of the *trans* configuration with respect to *cis*.[11,12,31,45] The *trans*→*cis* thermal isomerization is associated with different activation energy barriers depending on the protonation form of the chromophore:[32,33] data showed a much slower process

(40) Albertazzi, L.; Arosio, D.; Marchetti, L.; Ricci, F.; Beltram, F. *Photochem. Photobiol.* **2009**, *85*, 287–297.
(41) Jung, G.; Wiehler, J.; Zumbusch, A. *Biophys. J.* **2005**, *88*, 1932–1947.
(42) Jung, G.; Zumbusch, A. *Microsc. Res. Tech.* **2006**, *69*, 175–185.
(43) Dedecker, P.; Hotta, J.; Ando, R.; Miyawaki, A.; Engelborghs, Y.; Hofkens, J. *Biophys. J.* **2006**, *91*, L45–L47.
(44) Bosisio, C.; Quercioli, V.; Collini, M.; D'Alfonso, L.; Baldini, G.; Bettati, S.; Campanini, B.; Raboni, S.; Chirico, G. *J. Phys. Chem. B* **2008**, *112*, 8806–8814.
(45) Andresen, M.; Stiel, A. C.; Folling, J.; Wenzel, D.; Schonle, A.; Egner, A.; Eggeling, C.; Hell, S. W.; Jakobs, S. *Nat. Biotechnol.* **2008**, *26*, 1035–1040.

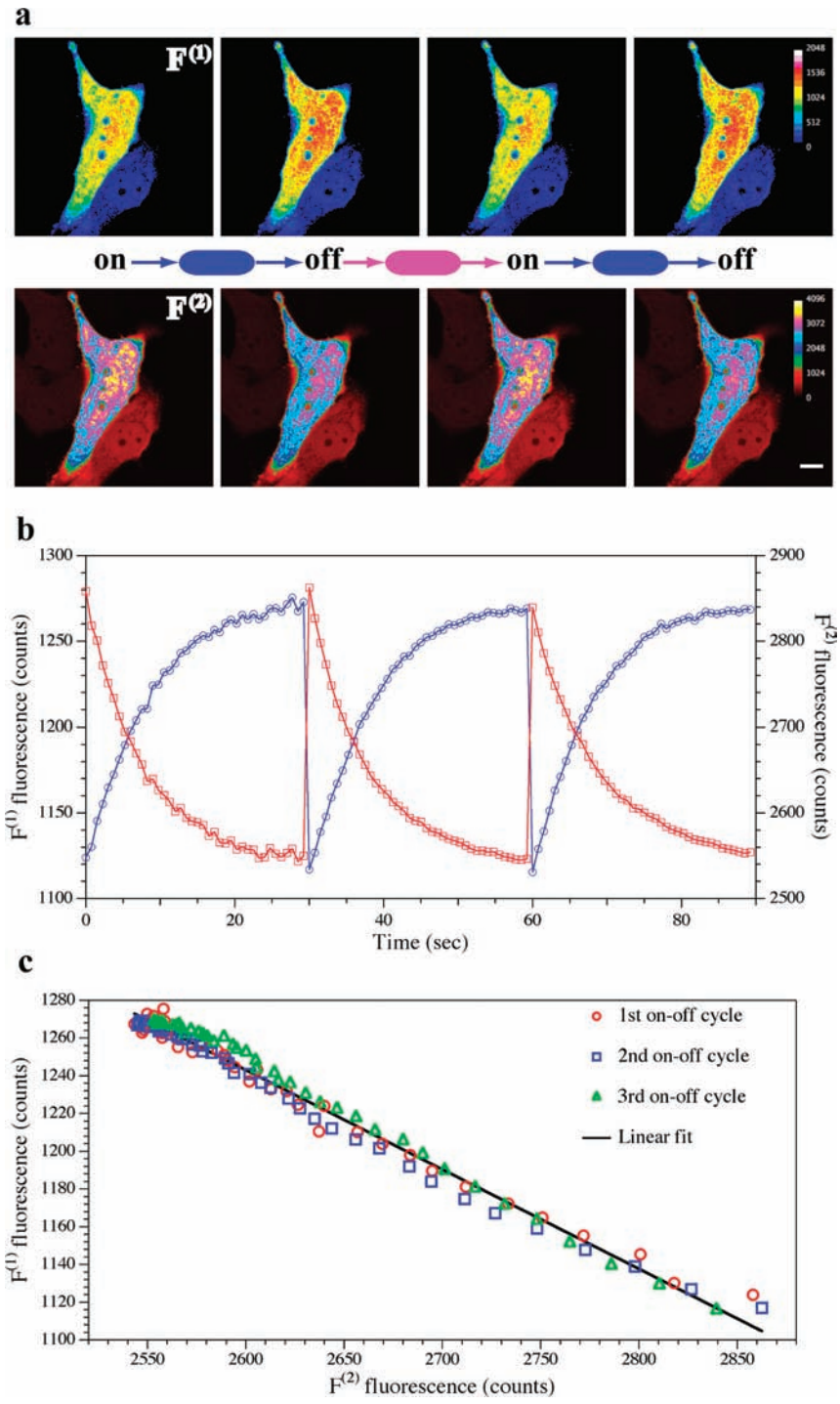

Figure 4. (a) Pseudocolor confocal images of the EGFP-L_{20}-EYQ1 fusion protein expressed in CHO cells. Upper panels: cell fluorescence collected in the $F^{(1)}$ (485−500 nm) emission range. Lower panels: cell fluorescence collected in the $F^{(2)}$ (509−525 nm) range. Note that the color scales are different. EYQ1 undergoes three photochromic cycles that affect FRET between the two protein. The "*off*" states (higher $F^{(1)}$, lower $F^{(2)}$) are obtained from the preceding "*on*" states (lower $F^{(1)}$, higher $F^{(2)}$) by excitation at 476 nm (15 kW/cm^2) for 30 s in scan mode. The *on* states are obtained from the preceding *off* states by excitation at 403 nm (1 kW/cm^2) for 20−30 s in scan mod. (b) Plot of $F^{(1)}$ (blue) and $F^{(2)}$ (red) fluorescence emissions for the three photochromic FRET cycles. Note that $F^{(1)}$ is mainly due to donor and shows a time-dependent saturable increase that parallels the decrease of $F^{(2)}$ (here the fluorescence increase of the donor cannot compensate the emission loss of the acceptor). (c) $F^{(1)}$ vs $F^{(2)}$ plot for the three photochromic FRET cycles displayed in (b). The black line represents the linear fit, which yields $E = 32 \pm 4\%$.

for the case of neutral chromophores with respect to anionic ones. Since the thermal decay (time scale: seconds−hours) is always much slower than the protonation reaction (time scale: ≤ms), we can safely assume that the latter is always at equilibrium. Consequently, our quantitative analysis of the thermal recovery rate versus pH yields the pK of the *trans* chromophore ionization (pK_t).

The *trans* isomer displays a much higher ionization pK (pK_t > 9.3) compared to its *cis* counterpart. It is very likely that the higher value of pK_t stems from a different chromophore

environment in the *trans* states that hinders proton relay reactions toward the external buffer. A similar condition is thought to hold also for photochromic Dronpa.[9] We can conclude that at physiological pH protonated A_t is the most stable *trans* ground state. This stability accounts for the large absorption shift to 400 nm and the decrease in fluorescence upon illumination of native B at pH < 9. The presence of a *trans* anionic state B_t is clearly demonstrated by pH-jump experiments after photoconversion at neutral pH (Figure 3d). We should note that these experiments demonstrate for the first time the existence of a protonation equilibrium involving the *trans* states in a photochromic FP, an elusive phenomenon previously discussed for other FPs on the basis of X-ray structures.[9]

Just like occurring for isolated AFP chromophores,[11] protein *cis*→*trans* and *trans*→*cis* chromophore photoisomerizations are single-photon processes. Optical excitation leads eventually to a photostationary state for which the *cis*→*trans* and *trans*→*cis* photoisomerization rates are the same. The isomer ratio at this photostationary state depends critically on the relative absorption and switching yields at the specific illumination wavelength (Figure 1c); the latter, in turn, depend on pH. Together with the illumination intensity, these parameters determine also the switching rate. The full reversible photoisomerization scheme (valid for a few cycles) is amenable to a simple modelization (Supporting Information) that relies upon the *intrinsic* switching yields for all states involved in the photoisomerization process (Table 1). Combined with the knowledge of the molar spectra of the four individual ground states, this model allowed us to estimate the intrinsic photoswitching yields of our mutants (Table 1) from the measured photoconversion curves (Figure 3b). Notably, previous attempts to measure intrinsic switching yields were made under ad hoc assumptions about the molar spectra of the photoconverted forms.[8] Conversely, our mutants display irreversible photobleaching yields in line with those reported for most AFPs[37] (Table 1). Collectively, these results show that the present mutants photoisomerize 2−3 orders of magnitude more efficiently than any reported photochromic AFP (Table 1). These values are similar to those reported for other valuable photochromic FPs such as Dronpa (Table 1).[8,43] Even if this work mostly focused on Mut2Q and EYQ1, we demonstrated efficient photochromism in the cell environment also for EQ1 (F64L/S65T/E222Q GFP) and EYQ2 (F64L/S65T/T203Y/E222Q). EQ1 is obtained just by introducing the single E222Q replacement in the primary sequence of "enhanced GFP" (EGFP, F64L/S65T GFP), arguably the most popular green FP in biophysical and molecular biology studies. This single-point transformation of EGFP may therefore represent a simple and straightforward solution to add a photochromic green reporter to already existing fluorescent protein constructs.

On account of these results, we should like to stress that the E222Q mutation translates into a significant improvement in the suitability of AFPs for imaging applications based on photochromic properties, although the intrinsic photoswitching yields measured for the isolated chromophore are still higher by 1−3 orders of magnitude (Table 1). Note, however, that super-resolution techniques such as FPALM or STORM will actually benefit by efficient but not too fast photoswitching rates. In these techniques, in fact, the resolution is intrinsically related to the number of detected photons per molecule, which are in turn strongly influenced by the photoswitching/photobleaching yields.[46] If the *off* photoswitching is too efficient, fluorescence read-out is temporally limited and only a few photons may be collected. Consistently, if the *on* photoswitching is very efficient, the chance that read-out illumination will photoactivate some dark molecules would increase. In both cases, we have a (possibly significant) decrease in the localization precision of the imaging method. Nonetheless, the residual hampering effects on chromophore photochromism by other protein residues in the folded structure is worth investigating, and we are currently devoting scientific effort to it. We should like to stress that the most severe limit to image acquisition from photochromic mutants, as well as conventional FPs, is irreversible photobleaching.[46] In this sense, our mutants display the same good stability of most AFPs (about 10^5 photons can be absorbed, and mostly emitted, prior to irreversible photobleaching).

Yellow EYQ1 and EYQ2 are very good candidates to play the role of acceptors in photochromic FRET schemes. Indeed, we were able to demonstrate that FRET between a green donor (EGFP) and EYQ1 is easily monitored in the cell by carrying out sequential *on*−*off* photocycles on EYQ1. This effect stems from the significant shift in the absorption spectrum determined by photoisomerization of EYQ1 from state B to A_t (B_t is not formed at physiological pH in the cell). Such a photochromic FRET scheme avoids all the experimental complications caused by donor−acceptor optical cross-talk and allows an accurate measurement of FRET efficiency. Notably, our model binary constructs EGFP-L_{20}-EYQ1 can be used as reference for FRET measurements in any conditions, as described in our mathematical treatment of photochromic FRET (Supporting Information).

Conclusions

The recent discovery of reversible and irreversible PAFPs is giving much impulse to new imaging strategies. The rapid diffusion of these new techniques among biophysicists and molecular biologists in turn prompts the development of new PAFPs tailored to specific in vivo applications. In this context, the lack of efficient photochromic variants belonging to the *Aequorea victoria* family (AFPs) is a major drawback, owing to the vast popularity of these molecules as genetic fluorescent reporters in fusion constructs for eukaryotic expression. Isolated AFP chromophores, however, are photochromic and the poor switching behavior reported so far in only few AFPs poses a stimulating question: can we design AFPs to limit or even eliminate this inhibitory effect? In this work, we demonstrate that the E222Q replacement strongly enhances the photochromic properties of AFPs. This effect was found to take place in four AFPs with different mutation patterns and optical properties and appears therefore quite general. E222Q AFP photochromic behavior was shown to derive from a *cis*−*trans* isomerization, analogously to the isolated chromophore case.

We identified the main spectroscopic and photophysical properties of the photochromic mutants. We should like to emphasize the demonstration of the subtle interplay between photochromicity and chromophore ionization and the quantitative determination of the switching yields of all ground states that involved in photoisomerization. Importantly, we found that switching in these mutants is 2−3 orders of magnitude faster than in all reported photochromic AFP. For what concerns the detected thermal recovery from *trans* states, we note that this process is very slow (hours) in the pH range typical of cell

(46) Gould, T. J.; Verkhusha, V. V.; Hess, S. T. *Nat. Protoc.* **2009**, *4*, 291–308.

experiments and will not perturb significantly the imaging techniques for which our mutants were tailored. Nonetheless, the recovery rate *does* depend on the mutation pattern, and we believe further studies may provide engineering strategies leading to photochromic AFPs free from thermal recovery.

Acknowledgment. We thank Prof. Erwin Neher, Dr. Riccardo Nifosì, Dr. Stefano Luin, and Prof. Gregor Jung for useful discussions, Dr. Pietro Amat for helping in the preparation of TOC graphic, and Dr. Samanta Raboni for helping in the preparation of the Mut2Q protein. This work was partially supported by the Italian Ministry for University and Research (MiUR) under the framework of the FIRB project RBLA03ER38.

Supporting Information Available: Kinetic analysis of protein *cis*/*trans* photoisomerization (theoretical model and experimental data analysis), analysis of FRET emission from a photochromic acceptor (theoretical model and experimental data analysis), Figure S1. This material is available free of charge via the Internet at http://pubs.acs.org.

JA9014953